



SPIRE Technical Report

Ref: SPIRE-RAL-REP-002983

Issue: 1.0

Date: 26-Oct-2007

Page: 1 of 12

SPIRE ILT Microvibe Report
Doug Griffin

Change Log

Date	Change	Issue
Friday, 26 October 2007	Initial release	1.0

Reference Documents

RD	Document	Comments
RD1	Herschel STM Micro-vibrations test Report H-P-2-ASP-TR-1110, Issue 2	
RD2	Herschel STM Micro-vibrations Analysis Report H-P-2-ASP-AN-0773, Issue 2	This document was updated from Iss. 1.0 to 2.0 after completion of the STM micro-vibration testing
RD3	Micro vibration analysis concerning optical instruments of Herschel spacecraft HP-ASPI-MO-218	
RD4	SPIRE Science Verification Review #3 SPIRE Bolometer Array Performance Document	

1. Table of Contents

Change Log	1
1. Table of Contents	1
2. Introduction	2
2.1 Pass / fail criteria	2
2.2 Test setup description	2
2.3 Spacecraft level testing and analysis	4
3. Instrument Input Acceleration Calibration	4
4. SMEC Susceptibility tests	7
5. Detector Susceptibility	8
6. Conclusions and recommendations	12



2. Introduction

Micro-vibration susceptibility tests were carried out during the PFM ILT-4 and ILT-5 test campaigns to investigate the behaviour of the SMEC Mechanism and the Photometer and Spectrometer detector systems. The thermal instrument interfaces must be compliant with the IID-B requirements in order to characterise the micro-vibration susceptibility characteristics of the instrument.

2.1 Pass / fail criteria

The effective pass/fail criteria for the SMEC mechanism micro-vibration immunity requirement is its ability of the feedback control loop to maintain the velocity and position requirements in the flight-like micro-vibration environment.

The effective pass/fail criteria for the Photometer and Spectrometer detector system is that there be negligible increase in the noise threshold of the detectors in the flight-like micro-vibration environment.

2.2 Test setup description

The micro-vibration disturbance was generated by a shaker which was connected to the chassis of the cryostat via a trunnion link (Figure 2). This input force induced a vibration response in the cryostat structure, optical bench and the instrument. The response of the optical bench was monitored by a tri-ax seismic accelerometer mounted close to the cone mechanical interface to the instrument. The accelerometer gave no signal at the cryogenic operating temperature of the instrument and therefore the acceleration levels at the instrument interface could not be measured directly. The approach taken was to characterise the response at the instrument interface at room temperature, under vacuum at a given coil current amplitude. The same current amplitude was used for both the room temperature system characterisation and the cryogenic susceptibility tests. The validity of this pragmatic approach to the test is limited by (1) the variation in the shaker to optical bench transfer function between room temperature and cryogenic temperature and (2) the stability of the shaker and coupling and its ability to create a reproducible disturbance level. The most significant factor of these two is judged to be the change in the stiffness of the thermally isolating mounting legs of the Herschel OBA simulator between room temperature and cryogenic temperature which will tend to increase the resonant frequencies of the system.

No attempt was made to modulate the amplitude of the input to achieve a flat spectral response at the SPIRE interface. As a consequence, the amplitude of the response at the SPIRE interface will be dominated by the resonances of the cryostat and instrument.

The range of frequencies investigated ranged from 20 – 80 Hz. This range covered the range of rotation frequencies of the reaction wheels, but not the higher frequency harmonics.

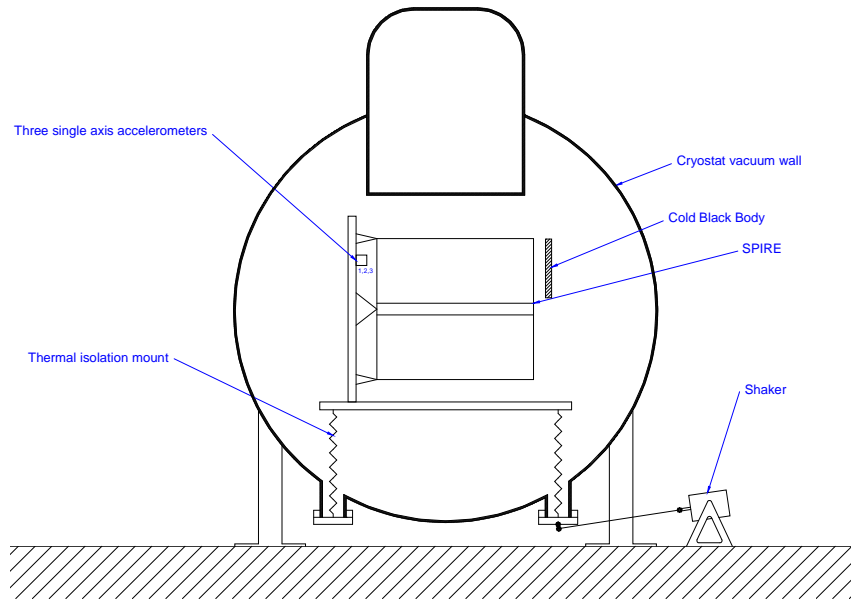


Figure 1 – Schematic representation of ILT test setup



Figure 2 - Portable shaker interfacing to the chassis of the ILT cryostat

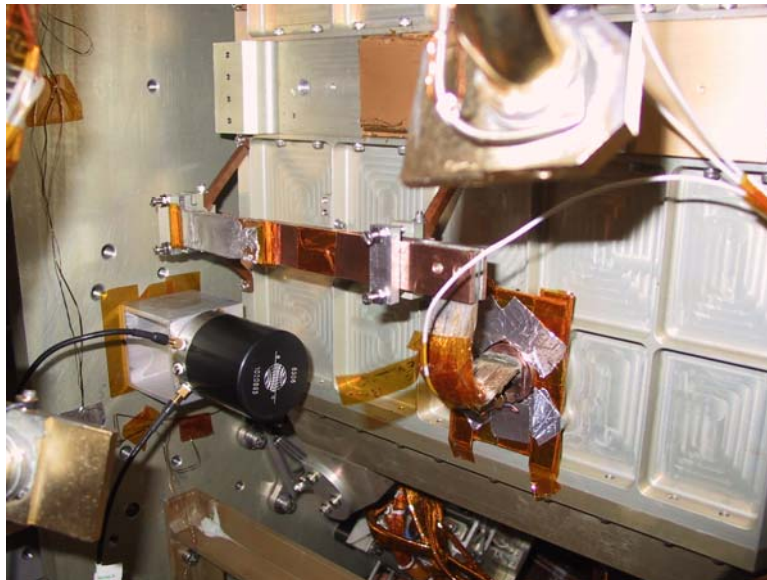


Figure 3 - Seismic tri-ax accelerometer mounted on the Herschel OBA simulator

2.3 Spacecraft level testing and analysis

A FEA model of the spacecraft to model the micro-vibrations induced into SPIRE by the reaction wheels has been produced by industry (RD2). This model has been validated during the Herschel STM test programme (RD1) and found to correlate well with the test results. Using the data from the reaction wheel supplier (TELDIX) and the FEA model, the expected acceleration at SPIRE is expected to be 96 mg.

3. Instrument Input Acceleration Calibration

As described above in §2.2, the acceleration level at the SPIRE mechanical interface was not measured at the cryogenic operating temperature of the instrument as the accelerometers ceased to work below $\sim 30\text{K}$. Figure 4, Figure 5 and Figure 6 show the response at the SPIRE interface when the cryostat was under vacuum and at room temperature for three separate orthogonal axes. Figure 7 is the quadrature sum of these three responses to yield the overall vector magnitude of the response. The maximum response level predicted in the spacecraft cryostat by RD2 is 96mg. In general the responses generated during the ILT micro-vibration tests were one to two decades below (20-40dB) these levels whereas the peak ILT response was ~ 3 times lower.

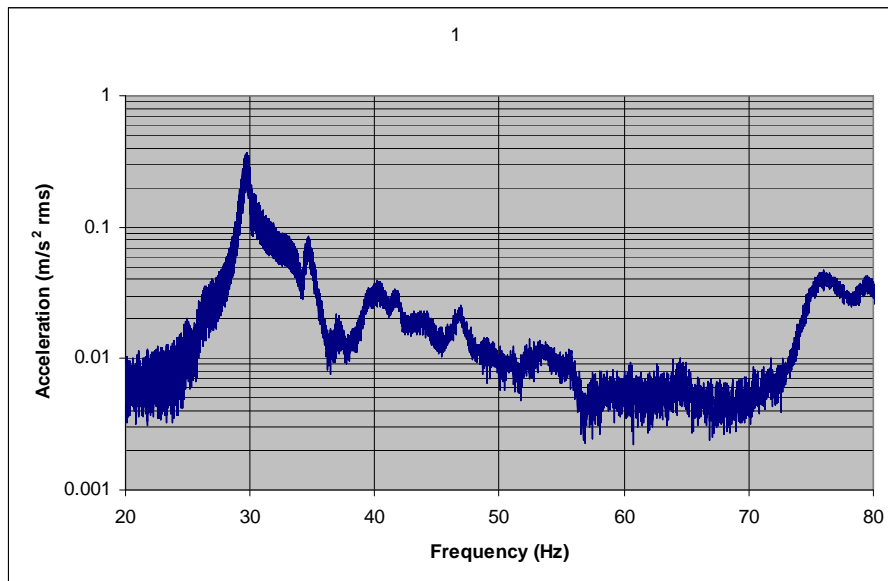


Figure 4— Vibration response at SPIRE interface in first axis during ILT tests.

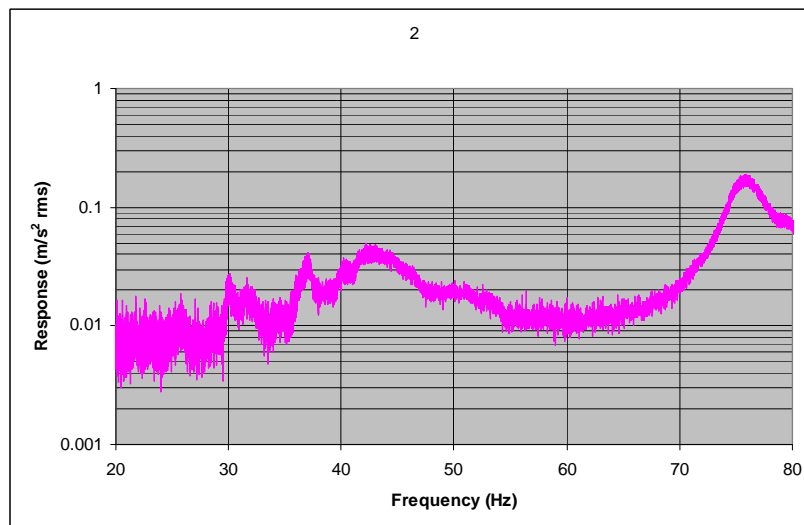


Figure 5 – Vibration response at SPIRE interface in second axis during ILT tests.

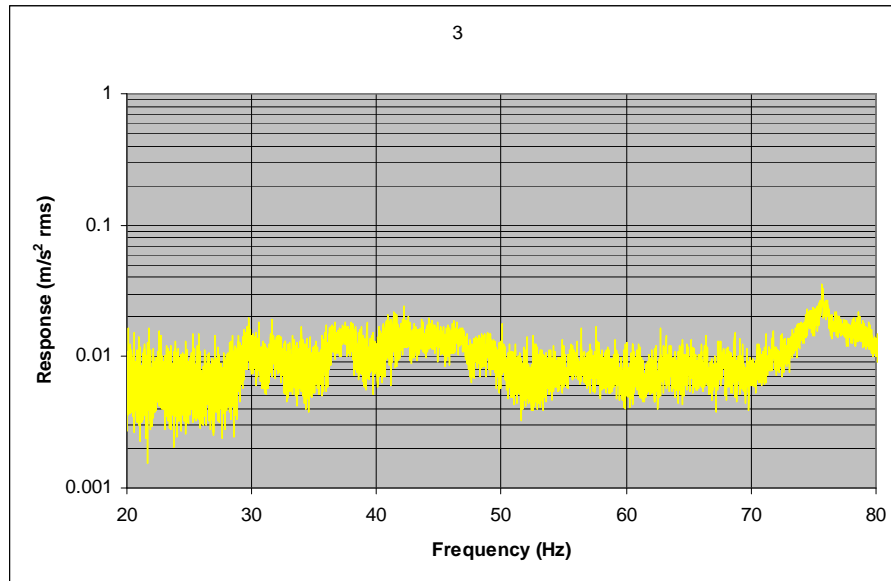


Figure 6 – Vibration response at SPIRE interface in third axis during ILT tests.

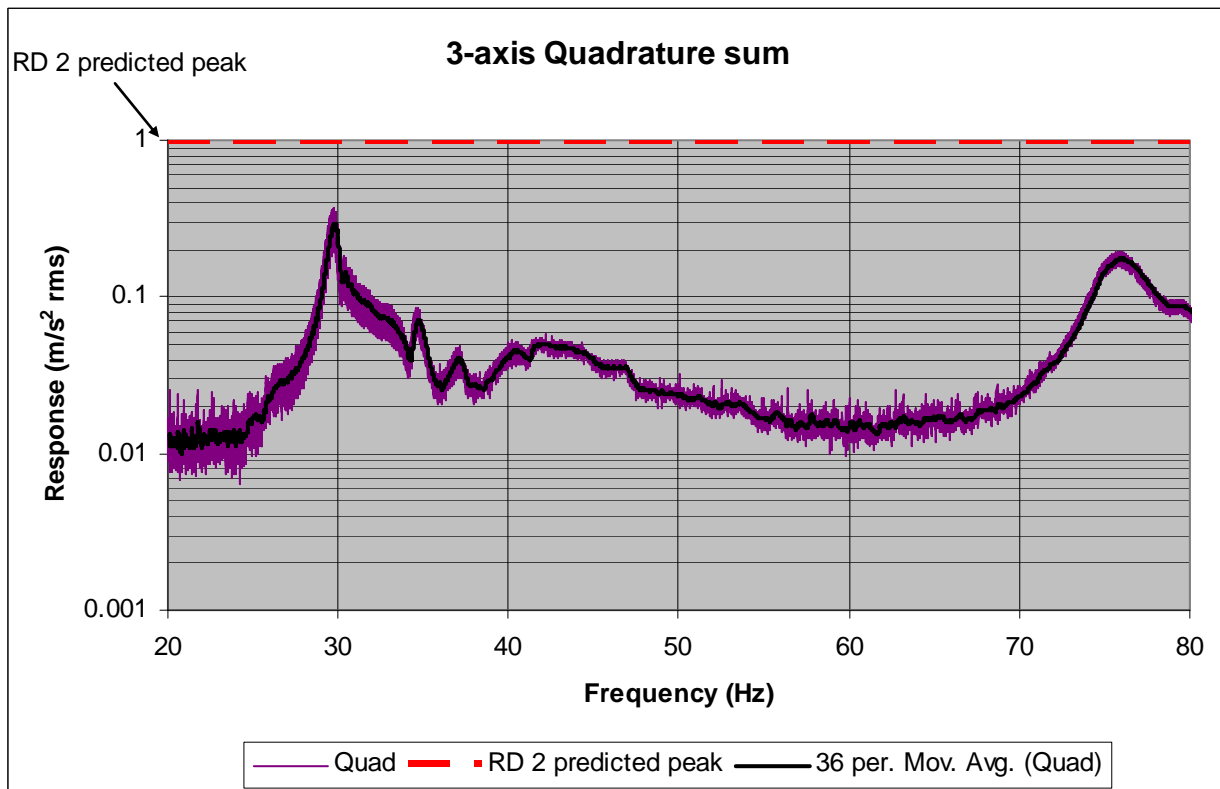


Figure 7 – Inferred acceleration magnitude vs. frequency for SPIRE ILT micro-vibration tests. The predicted maximum amplitude of the acceleration at the SPIRE interface as predicted by Thales analysis (RD2) is indicated by the red dashed line.



4. SMEC Susceptibility tests

Figure 8 shows the error in the SMEC trajectory position for two series of SMEC scans. The first test (Obsid: 0x300114C8) was a set of high resolution scans carried out without any vibration input to the cryostat. The second scan shows the same information during a series of 20-80 Hz micro-vibration sweeps.

The effect of the micro-vibration disturbances on the SMEC velocity error is shown in Figure 9. The micro-vibration disturbance was a constant 60Hz for these tests. The test was conducted at a scan speed of 250 $\mu\text{m/s}$ and 500 $\mu\text{m/s}$ and compared with a reference scan with no micro-vibration disturbance. The acceleration level during this test was in the order of 1-2 mg.

There is no evidence that the micro-vibration disturbances seen during the tests degraded the performance of the mechanism.

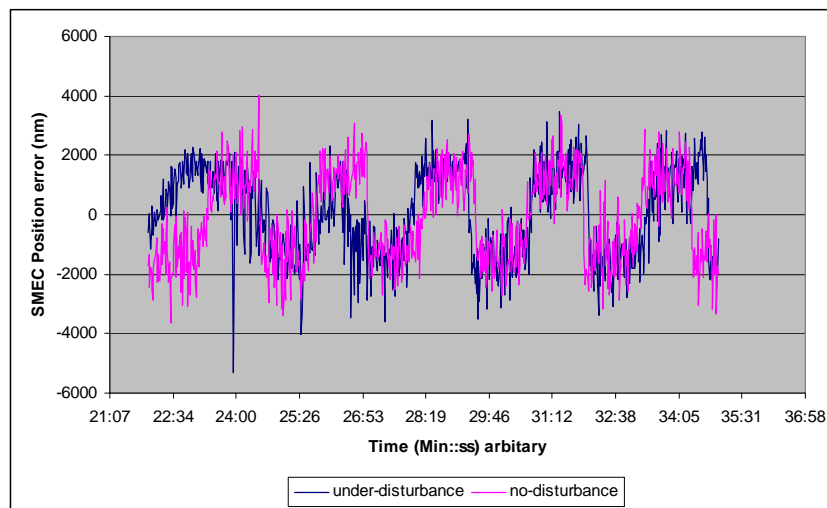


Figure 8 – SMEC Position error under the influence of the

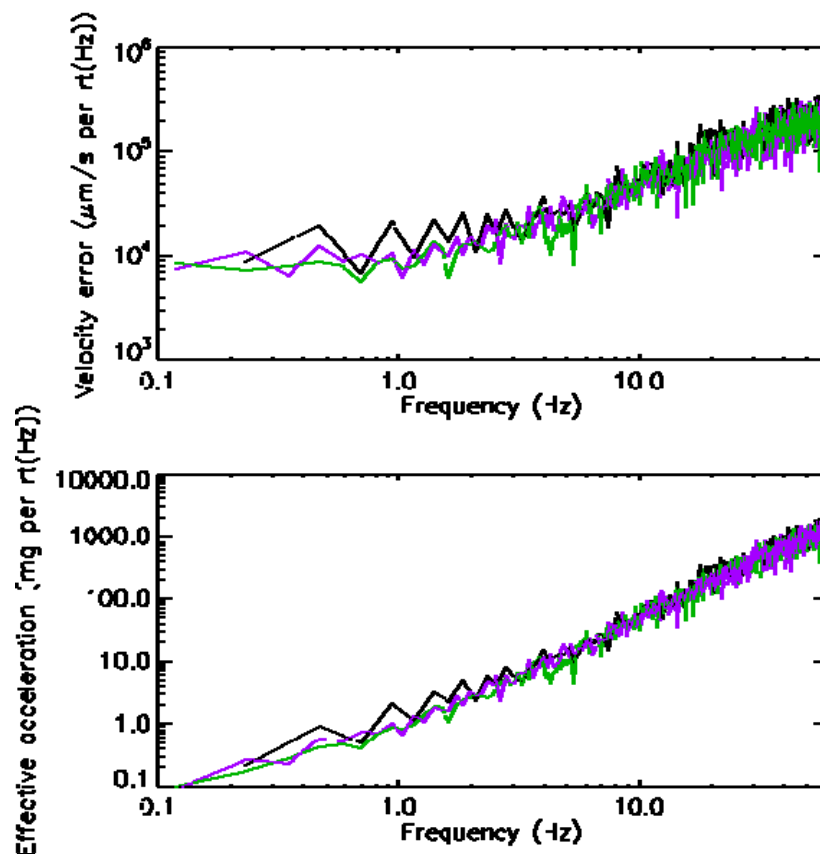


Figure 9 – Power spectral density of the velocity error of the SMEC (top) and the corresponding stage acceleration (bottom). The Black trace is a scan without an applied micro-phononic disturbance; the Green trace is for a stage speed of 500 $\mu\text{m/s}$ under 60 Hz disturbance (0x3001150D); the Purple trace is a 250 $\mu\text{m/s}$ stage speed under 60 Hz disturbance (0x3001150E).

5. Detector Susceptibility

The SPIRE detectors are readout with lock-in amplifiers which are sensitive to signals at the bias frequency of the detectors (\pm the amplifier output LP filter bandwidth) as well as the odd harmonics of the bias frequency. The bias frequency of the detectors can be tuned to move the detector signal away from frequencies which demonstrate a high level of microphonic susceptibility. To test the efficacy of this mechanism, tests were carried out with broadband white noise (10-1000 Hz) disturbance. The level of this disturbance is un-quantified but is likely to be less than 96 mg. The SPIRE Science Verification Review #3, SPIRE Bolometer Array Performance Document (RD4) contains analysis of tests carried out on the susceptibility of the detectors. The reader is directed to this document for the details of this analysis. The conclusions from this analysis are reported in Figure 10 in order to summarise the results of this analysis in this summary document. The results indicate that microphonic noise on the detectors is a strong function of the detector bias frequency, and therefore it has been demonstrated that adjusting of the detector bias frequency is a useful technique for mitigating the effects of micro-vibrations. As the structural response of the instrument in the ILT cryostat will be different to the response in the flight cryostat, the susceptible bias frequencies identified in these tests will almost certainly be different in the flight cryostat.



The main conclusions are as follows:

1. At a single bias frequency, the microphonic response is repeatable and decreases with decreasing resistance.
2. Individual microphonic features often do not repeat as the bias frequency is changed, under the assumption that the features are located near the first harmonic of the bias frequency. This indicates that many of the features are located near higher, odd harmonics.
3. Channels 1-24 in the short-wavelength spectrometer have the greatest microphonic response, followed by channels 25-42 in the short-wavelength spectrometer. The microphonic response of the long-wavelength spectrometer is an order of magnitude lower.
4. For the spectrometer the worst microphonic response is observed for bias frequencies between 230 and 300 Hz. The region near 200 Hz appears to have the least response.
5. For the photometer the worst microphonic response is observed for bias frequencies between 130 and 180 Hz. The region near 125 Hz appears to have the least response.

Figure 10 - Conclusions on the results on the detector microphonic tests (taken from RD4).

Figure 11 shows the spectra obtained when the input disturbance was being constantly swept between 20 and 80 Hz at constant amplitude and also a comparison with spectra obtained under the same conditions without input disturbance. The degradation in the SNR is marked under these conditions. The error in the SMEC position was seen to be not affected by the disturbance, and therefore the degradation was seen to be due to the pickup on the detectors.

Figure 12 shows the spectra obtained during a series of scans with the disturbance tuned to 40 Hz and 60 Hz. This pick up on the detectors can be seen as an anomalous spike in the spectra in the detectors in the lower half of the array. The effect of changing the frequency of the disturbance is to shift the apparent optical wavelength of this anomalous spectral feature.

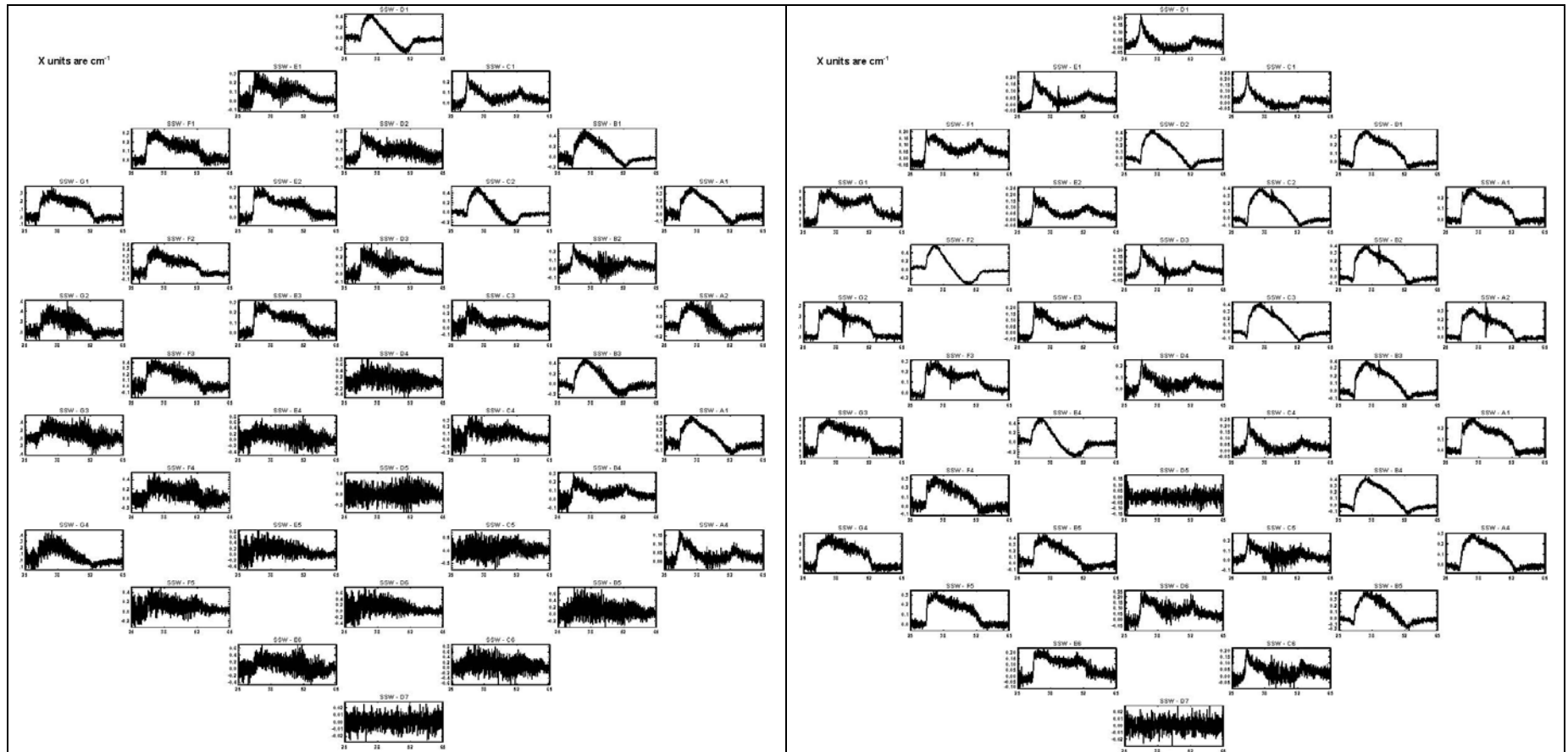


Figure 11 – [Left] Spectra obtained from the SSW array during the application of a micro-vibration disturbance to the ILT cryostat (20-80Hz sweeps) [Right] Spectra obtained from the same array with the same detector parameters without disturbance. (ObsID: 0x30011500)

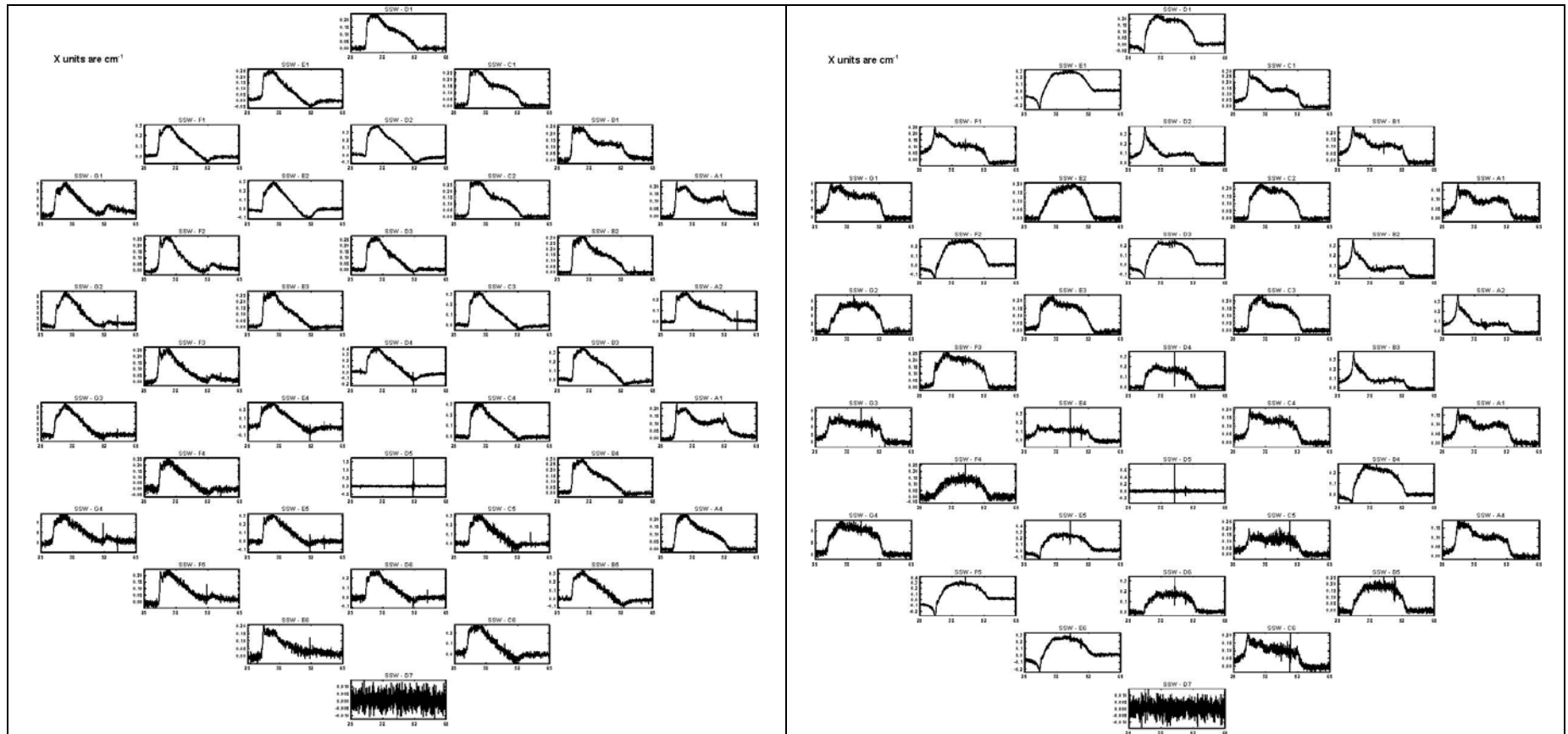


Figure 12 - [Left] Spectra obtained from the SSW array during the application of a 60 Hz micro-vibration disturbance to the ILT cryostat with a [Right] Spectra obtained from the same array with the same detector parameters without disturbance. (ObsID: 0x30011500)



6. Conclusions and recommendations

General

1. The calibration results indicate that the amplitude of the micro-vibration disturbance generated in the ILT cryostat was significantly lower than the levels predicted in the analysis in RD2.
2. Under the disturbance levels generated during the ILT tests, the SMEC saw no perceptible degradation in performance
3. Under the disturbance levels generated during the ILT tests, the noise performance of the detectors saw a marked degradation
4. The ability to tune the detector bias frequency away from was demonstrated to be effective in ameliorating the noise performance degradation

Spacecraft testing

Given the fact that susceptibilities in the detector have been identified and the micro-vibration environment in the spacecraft cryostat will be significantly different to the ones induced during the ILT microvibration tests, viz;

1. The amplitude of the disturbances will be different. If the ILT calibration approach is valid and there are no hidden margins in the analysis, then the levels in flight will be higher, and
2. The spectral content of the disturbances will be different due to the nature of the input and the structural transfer function between the reaction wheels and the instrument interface;

the behaviour of the instrument in the presence of the flight-like disturbances needs to be prioritised.

The principal aims of these tests are to;

1. Quantify the level of susceptibility seen in the flight-like environment
2. Identify any constraints on spacecraft operations where SPIRE is particularly susceptible
3. Quantify the amount by which the detector susceptibilities can be avoided by tuning the detector bias frequency

It would be important to have sufficient time with the spacecraft in the horizontal position to be able to run the tests with the SMEC in scan mode.

It would also be important to model as faithfully as possible by suspending the spacecraft during the tests to remove the effects of the spacecraft MGSE dolly on the amplitude and spectral environment response at the instrument interface.

Modelling

Linking the planned scenarios for operational reaction wheel use, the actual static and dynamic imbalances of the reaction wheels obtained during acceptance testing and the structural transfer function between the reaction wheels and the instruments prior to the spacecraft testing would give useful information to enable SPIRE to select detector bias frequencies away from the principal structural response frequencies.